Tribology of Shearing Polymer Surfaces. 1. Mica Sliding on Polymer (PnBMA)

M. Heuberger,[†] G. Luengo,[‡] and J. N. Israelachvili*[,§]

Materials Department, ETH, 8092 Zürich, Switzerland, Physical Chemistry Department, Complutense University, Madrid, Spain 28040, and Department Chem. Eng. and Materials Department, University of California, Santa Barbara, Santa Barbara, CA 93106

Received: March 30, 1999; In Final Form: September 22, 1999

The energy-dissipating processes associated with shearing polymer junctions were investigated at the molecular, microscopic, and macroscopic levels using the surface forces apparatus−FECO optics technique. For a solid surface of mica sliding across a polymer surface of poly-*n*-butyl methacrylate (PnBMA) at low sliding velocities and at temperatures close to the glass transition temperature, $T_g = 25$ °C, the friction was mainly of the stick−slip variety; the static friction force F_s was always high and remained relatively constant, attaining its equilibrium steady-state value immediately on commencement of sliding, but the kinetic friction force F_k decreased from an initially high value to a very low value as sliding progressed. The friction forces exhibit complex time, temperature, load, and velocity dependencies and cannot be properly described in terms of a single parameter such as a "friction coefficient" or "shear stress". These, and other tribological characteristics of this type of system, appear to be very different from those of hard surfaces or simple liquid-lubricated surfaces. Where comparison with literature data is possible, the tribological results on these molecularly smooth "model" surfaces are similar to those for "engineering" surfaces sliding on bulk polymer. The molecular mechanisms and relaxation processes responsible for the observed tribological behavior and adhesion hysteresis of this type of system (solid surface sliding on polymer) are discussed at the end of this and the accompanying paper on the complementary system of polymer sliding on a solid surface of mica.[1]

Introduction

Polymers are used as low-friction materials, coatings, or lubricating fluids in a growing number of mechanical devices where low adhesion, friction, and wear are important factors for determining performance and lifetime. The polymer surface may slide against another polymer surface (symmetric system, Figure 1a) or against another material (asymmetric system, Figure 1, parts b and c). Asymmetric tribological systems, which are the focus of this and a subsequent paper,[1] have not been as systematically studied with the surface forces apparatus (SFA) technique as have symmetric systems,[2−5] and to our knowledge no asymmetric tribological polymer system has so far been investigated using this technique.

In an asymmetric system, one must distinguish between the sliding surface and the nominally stationary substrate surface. The difference between these two configurations is illustrated in parts b and c of Figure 1. In Figure 1b, as the slider moves relative to the substrate, it forms a friction track on that surface (i.e., on material B), but the friction track (or friction "spot") remains at the same location on the slider surface (of material A). Interchanging the surfaces or the materials of the two surfaces will now leave a track on the surface of material A (Figure 1c), which could be very different from the track left on the surface of material B (Figure 1b). In general, these two distinct configurations may be expected to exhibit very different tribological properties. This intrinsic duality of asymmetric systems adds a new degree of complexity that does not exist in symmetric systems (Figure 1a). Therefore, we have decided to split the results into two parts. This paper (part 1) considers a solid surface of mica (the slider) shearing across a polymer substrate (A sliding on B). Part 2 of this study[1] describes the results of the other configuration (B sliding on A) and compares the two.

The low friction coefficients (0.01−0.3) of polymer surfaces have been appreciated by engineers for many years .[6] It is now well established that the friction of polymer surfaces depends strongly and often nonlinearly on many parameters such as the sliding velocity, temperature, degree of confinement (load), and other time-dependent and "history" effects.[7] These tribological properties have been attributed to various molecular relaxation mechanisms occurring at different characteristic distance and time regimes.[8]

Using an SFA coupled to the FECO optical imaging technique, it was recently shown that the energy dissipation or "adhesion hysteresis" of two polymer surfaces during an adhesion−separation cycle involves both viscous flow on a microscopic scale and molecular scale interdiffusion across the interface.[9] Such adhesion hysteresis effects are expected to be related to the friction forces which often involve similar relaxation processes.[10]

Experimental Section

Measurements were performed with an SFA which allows one to control and measure the distance and normal force or load between two surfaces. The load L is determined from the deflection of springs of spring constant k_L and the distance D between the surfaces is measured using multiple beam interferometry (MBI).[11]

For the friction measurements, we used a friction attachment[3] inside the SFA that allows one to drive the upper surface past

[†] ETH.
[‡] Complutense University.
[§] University of California, Santa Barbara.

10.1021/jp991098a CCC: $18.00
Published on Web 11/03/1999

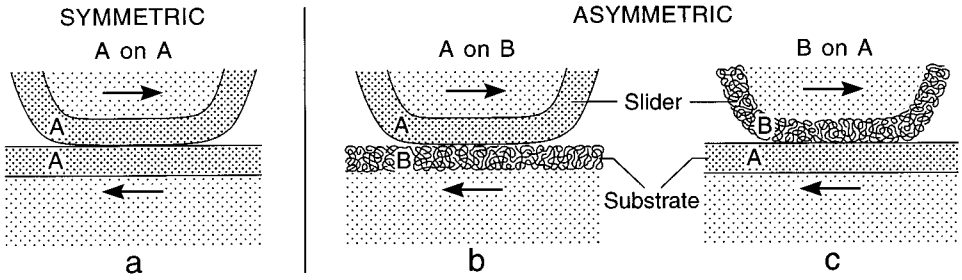

Figure 1. Symmetric and asymmetric polymer surface configurations. Here we describe results obtained for configuration b where a smooth mica surface slides across a stationary polymer (PnBMA) surface. In a subsequent paper,[1] we describe the results of a similar study for configuration c.

the lower surface while simultaneously recording the lateral or friction forces. In this case, the drive mechanism was a reversible DC motor connected to a horizontal micrometer screw that pressed against a slider held by a double-cantilever spring. This ensured linear horizontal motion of the slider. The slider was linked via two vertical friction-force-measuring springs to the stage supporting the upper surface. The friction force, F, was measured with strain gauges attached to the friction-force-measuring springs. The inertia of the moving stage, which is an important factor in determining tribological transient effects such as stick−slip behavior,[13] is characterized by the mass of the stage, m, and the stiffness of the friction-force-measuring springs, k_F. The signal (voltage) output from the strain gauge bridge is then recorded as a function of time on a chart recorder, storage scope, or computer to give the "friction trace".

To ensure a well-defined contact geometry, the surfaces were arranged in the shape of two crossed cylinders. Both surfaces were prepared from ∼3 μm thick sheets of mica glued onto cylindrically shaped silica glass disks. One of the two surfaces (the lower, stationary surface) was coated with a 0.3 μm thick layer of poly(*n*-butyl methacrylate), $[CH_2C(CH_3)(COO(CH_2)_3CH_3)]_n$ (PnBMA). The PnBMA layer was solvent cast onto mica from a 6 wt % solution of PnBMA in methyl ethyl ketone (MEK) by pulling the mica surface slowly out of the solution at a speed of 33 μm/s parallel to the cylinder axis. The PnBMA surface was then annealed in a vacuum for 3 h at 60 °C. The PnBMA has a molecular weight of $M_w = 33\ 7\ 000$ and a glass transition temperature of $T_g \approx 25$ °C. The carboxyl group butyl side chains extend roughly 1 nm from the backbone when fully stretched.

Multiple beam interferometry (MBI)[11] was used to measure the surface topography and separation through analysis of the fringes of equal chromatic order (FECO). To optimize the FECO sensitivity, we evaporated either 8 or 55 nm thick layers of silver as the reflecting mirrors on the back surfaces of the mica sheets. The silvered faces were then glued onto the silica disks using a sugar glue (a 1:1 mixture of dextrose and D-galactose). One surface was then chosen for the solvent casting process described above. We used a silver layer of 55 nm to visualize the "primary" FECO fringes and a 8 nm layer to visualize the "secondary" and "tertiary" fringe patterns which together allowed us to fully analyze the changing PnBMA topography in situ during the experiments.[11]

The smoothness of the polymer layer was ascertained by AFM and FECO interferometry (MBI) and found to be <3 Å RMS with isolated islands of height 10−20 Å. We may note that the effect of roughness on friction can be dramatic for *hard* surfaces because the "real" contact area can be well below the geometrical or "apparent" area, but polymers are usually sufficiently soft that their adhesion deforms the asperities, pulling them together so that the real contact area is the same as, or exceeds, the apparent area. This has been confirmed via adhesion measurements for a number of different polymer surfaces[27] including PnBMA surfaces.[9]

The upper cylindrical surface was driven parallel to the upper cylinder axis, i.e., perpendicular to the lower cylinder axis. This arrangement ensured that the contact area remained fixed in space during sliding and that the optics beam stayed aligned, centered, and in focus.

For each new friction force measurement, a new contact region was chosen by repositioning the surfaces in the x and y directions (this was done with the surfaces well separated by many micrometers, i.e., not in contact). Figure 2 sketches the general scheme of the friction measurements. Using the DC motor driver, the ∼50 μm mica contact diameter is displaced on the lower polymer surface along a ∼1000 μm path (starting at the center defined by $x = 0$). The positive x-axis defines the initial sliding direction.

Three independent experiments were carried out in a sealed SFA chamber at 0% relative humidity. Prior to each measurement, the apparatus was purged with dry nitrogen gas for at least 12 h. The temperature during measurements was controlled by thermostating the whole room to ±0.1 °C. The white light (for MBI) was IR-filtered using a 1 cm thick water filter to reduce heating of the surfaces. The effective temperature of the samples was typically 1−2 °C above the controlled room temperature, T.

Theoretical Background

Energy dissipation, such as friction or wear, is an inherently nonequilibrium process. To describe such processes, it has become common to use the concept of the dimensionless *Deborah number*, De,[12] which is defined as the ratio of the characteristic molecular or microscopic "relaxation" time of a process or system τ_c to the "observation" or "experimental measurement" time τ_{exp} during which the system is studied or measured. At a sliding interface, there is usually also a characteristic length scale, D_c (e.g., the molecular length, grain, or asperity size), which together with the characteristic relaxation time defines a characteristic sliding velocity as

$$V_c = D_c/\tau_c \tag{1}$$

The Deborah number can also be expressed as the ratio of the characteristic velocity to the actual experimental sliding velocity by

$$\mathrm{De} = \tau_c/\tau_{exp} = V/V_c \tag{2}$$

which is convenient for friction experiments. Maximum energy dissipation (friction force and mechanical-to-heat energy transfer) is usually observed at sliding velocities where De ≈ 1, i.e.,

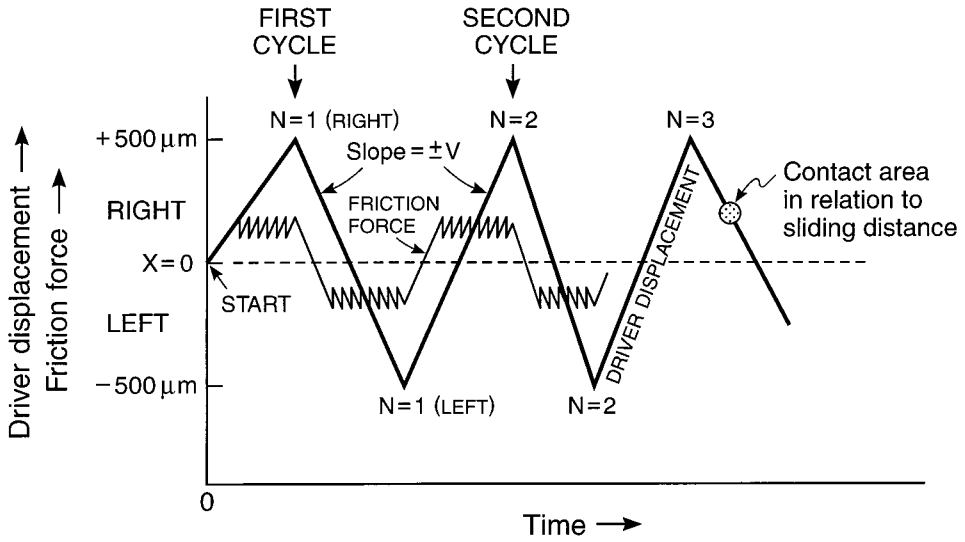

Figure 2. Experimental scheme used to slide the asymmetric system. The contact area has a typical diameter of 50 μm and moves along a friction track on the polymer substrate. The friction track has a total length of 1000 μm, i.e., 20 times the contact diameter. The sliding cycles start at the center at $x = 0$ (thick solid line), and each return passage over a given position on the polymer surface increases the cycle number N by 1. The measured friction force is shown by the thin line and is described in more detail in Figures 3 and 4.

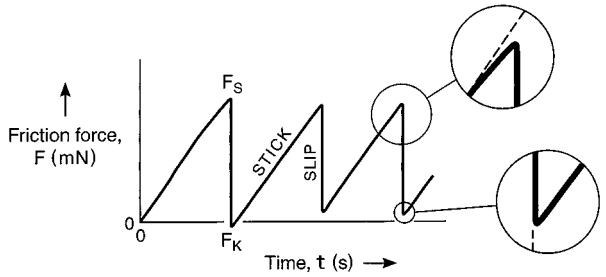

Figure 3. Typical stick−slip friction trace of the asymmetric system, mica sliding on PnBMA. The friction force F, which is proportional to the deflection of the friction force-measuring spring of stiffness k_F, is recorded as a function of time, t (see also Figure 2). The inset reveals that plastic flow already occurs in the *stick* phase before the surfaces *slip*.

when $\tau_{exp} \approx \tau_c$ and $V \approx V_c$. A reduction of V below V_c (corresponding to De < 1) brings the system closer to thermodynamic equilibrium and therefore to less energy dissipation, while at higher velocities (De > 1) the motion is too fast for efficient energy exchange to occur.[10] One can also define a critical velocity v_c ($v_c > V_c$) above which stick−slip motion changes over to smooth sliding. Many factors influence v_c such as the inertia of the stage (m and k_F), the driver velocity, V (or frequency or shear rate), and the applied load or pressure.[13] Real systems often have multiple relaxation processes, each associated with a different relaxation time so that the friction force can exhibit multiple peaks and valleys.[4]

Results

Friction Forces: Stick−Slip Sliding. Depending on the sliding velocity V and inertia of the stage, we observe smooth or stick−slip sliding. The stick−slip disappears above some critical velocity, $v_c > V_c$, above which one observes smooth sliding. The experiments presented here were performed both below and above the critical velocity, but mainly in the stick−slip regime. The typical shape of the recorded friction trace is displayed in Figure 3 which shows a measured friction force (F) versus time (t) at a constant driver velocity (V). We distinguish between the static and kinetic friction forces, F_s and F_k;[16] the static force F_s is given by the *measured* maximum force at the top of the *stick* portion of a stick−slip cycle, while the kinetic force F_k is the measured minimum value at the bottom of the *slip* portion of the cycle. During smooth sliding, the kinetic friction force F_k is defined as the friction force during steady-state sliding (i.e., when $F = F_s = F_k$). In this paper, in keeping with convention,[16] we use the same term "kinetic friction" for these two different types of friction, but we distinguish between the measured kinetic force during smooth sliding, where $F_k(\text{meas}) = F_k(\text{true})$, and the measured value during stick−slip sliding, where in general $F_k(\text{meas}) < F_k(\text{true})$.[13,14] Our friction traces indicate that the system is slightly "underdamped", which means [cf. ref 13] that $[F_k(\text{meas}) + F_s(\text{meas})]/2 > F_k(\text{true}) > F_k(\text{meas})$. Since $F_s(\text{meas})$ remained fairly constant, the measured values of F_k accurately reflect the trends in the true values of F_k.[16]

The inset in Figure 3 shows that the plastic yield stress is reached before the slip. The deviation of the friction force from a straight line already in the stick regime is indicative of a slow molecular relaxation mode, or "creep", which is estimated to have a relaxation time $\tau_\backslash$ of order 1 s. The possibility of the existence of other relaxation modes in this system is considered in the light of additional results.

Friction forces were also measured as a function of driver velocity, load, and temperature. The general stick−slip behavior of the system is reproduced schematically in Figure 4 as a function of sliding cycles (N), which is roughly proportional to the sliding time (t) and total distance traveled (x). The results show that the *static* friction force F_s undergoes no dramatic change as sliding proceeds from rest until the steady-state value is reached after a few cycles. In contrast to the weakly changing static friction force with time or sliding velocity, the *kinetic* friction force, F_k, exhibits a precipitous decrease over the first few cycles, eventually settling at a considerably lower value. We refer to this regime as the "transition" to steady-state sliding.

The Transition to Steady-State Sliding. By monitoring the MBI fringes, there was no detectable change of film thickness during transitions to steady-state sliding within a few angstroms at temperatures below 20 °C. This does not rule out smaller thickness changes, either shear thickening (dilation) or shear thinning, which generally does occur when a film is sheared. The near constancy of the film thickness suggests that any

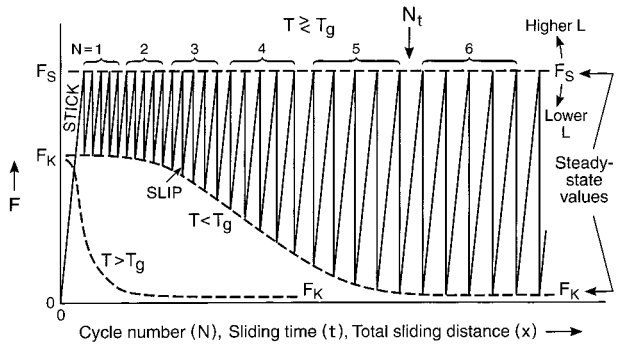

Figure 4. Schematic friction traces showing the transition from rest ($t < 0$) to steady-state sliding as a function of time at temperatures above and below T_g and at driver velocities, V, below the critical velocity, v_c. We may note that F_k exhibits a significant reduction during the transition while F_s remains largely unchanged.

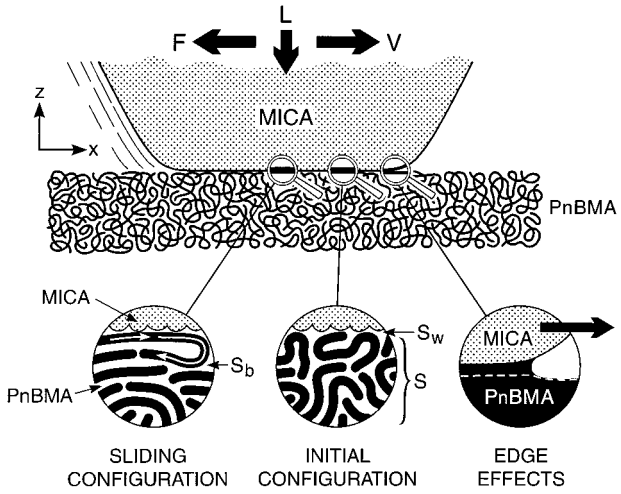

Figure 5. Simple molecular picture of the shearing solid−polymer interface showing the locations where slip can occur, either totally or partially: *wall slip* at S_w, *boundary layer slip* at S_b, and *film slip* or *bulk viscous slip* at S, which has no definite "slip plane" but a continuous shear gradient across the film. The results suggest that polymer alignment occurs at the interface in a way that lowers the kinetic but not the static friction forces.

changes occurring at the polymer surface involve in situ rearrangements of the molecules rather than material transfer (bulk flow) into or out of the contact zone. This is illustrated schematically in Figure 5.

To further elucidate the dynamics of the transition from rest to steady-state sliding, stop−start experiments where carried out where the sliding was stopped for a fixed period of time (with the surfaces remaining in contact under the same load) and then restarted at the same driver velocity. The aim was to see how quickly F_k relaxes back to its original (starting) value. However, no such relaxation in F_k was observed for stopping times ranging from 1 min to 12 h. This further suggests that, once the molecules at the shearing interface have become reorganized or shear-aligned into their kinetic sliding configuration, they do not quickly relax back to their original state once the sliding is stopped. The transition to steady-state sliding may therefore be thought of as a transition of the surface molecules to some shear-aligned "glassy" state and is similar to the behavior seen with certain branched hydrocarbon liquids that are used as base oils,[15] but unlike simple liquids that do relax very quickly to their original configuration once sliding is stopped.[14] The relaxation time τ_2 for this second-type of transition in F_k must be very long.

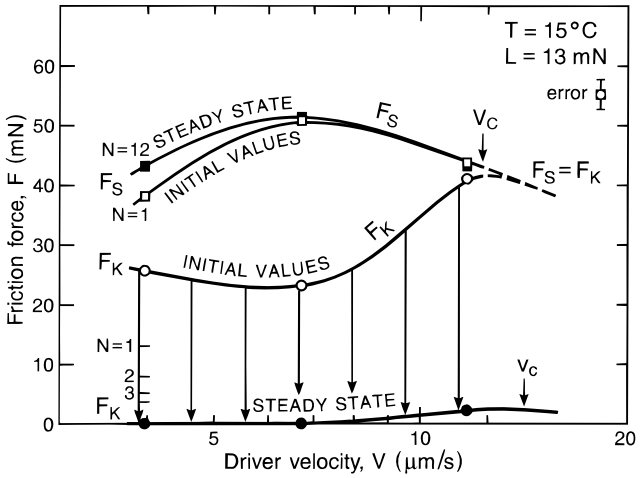

Figure 6. Data showing how the static and kinetic friction forces vary with time during the transition (indicated by the vertical arrows) from rest to steady-state sliding as a function of the driver velocity V at constant load and temperature. We may note the various maxima and minima in the curves, which are indicative of more than one relaxation mechanism.[4,10]

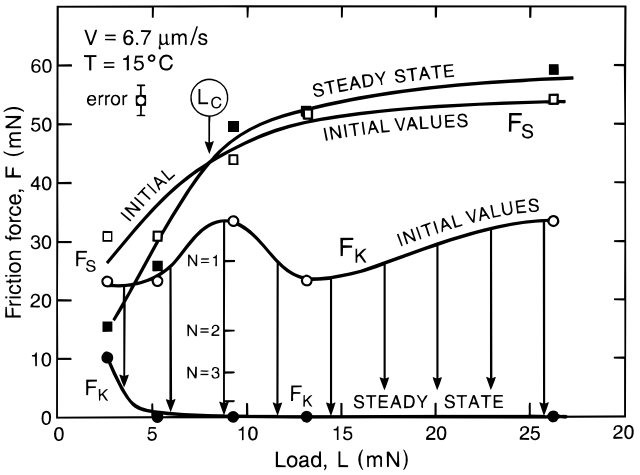

Figure 7. Similar data to Figure 6 showing how the static and kinetic friction forces vary with time during the transition as a function of the load L at constant velocity and temperature. The friction maximum with load arises from its dependence on confinement which can exhibit maxima at particular values of V, T, and L.[7] Typical pressures were, at $L = 5$ mN, $P \approx 1.6$ MPa.

Figures 6 and 7 show how F_s and F_k approach their equilibrium (steady-state) values with time at different driver velocities and loads. We may note that the static and kinetic friction forces display very different dynamic behaviors; the static force, F_s, does not change dramatically during the transition to steady-state stick−slip sliding. However, F_s increases slightly with time at low velocities and high loads but decreases at high velocities and low loads. Unlike F_s, F_k undergoes dramatic changes during the transition, generally decreasing to very low values after a few cycles, as already indicated in Figure 4.

The slight increase in F_s with sliding speed at low V is consistent with the observed creep relaxation, with increasing V the surfaces have less time to relax in the stick regime and so attain a higher yield force before slipping.[34] In the steady-state, F_s exhibits a maximum at a particular driver velocity near 7 μm/s in Figure 6, and above the characteristic velocity of ~10 μm/s the static and kinetic friction forces meet. This occurs near the critical velocity for stick−slip v_c for this system which, as expected, is also close to the characteristic relaxation velocity

V_c at which the friction force is a maximum. In Figure 6, F_k also exhibits a local *minimum* at about the same velocity as where F_s has its maximum. This is suggestive of the presence of other dissipation maxima (relaxation processes) at both higher and lower velocities.[4,10,13]

The slow creep observed in the stick phase (Figure 4), the freezing of the chains on stopping, the existence of a friction force *minimum* and the suggestion of two maxima in Figure 6, and the existence of a critical stick−slip velocity v_c at higher speeds[14] point to at least two relaxation mechanisms, a slow and a fast one, with relaxation times $\tau_2 \gg \tau_1$ that are at least 2 orders of magnitude apart.

In Figure 7, one finds a crossover point at a certain load L_c below which F_s decreases during the transition and above which F_s increases; that is, at L_c the static friction force does not change during the transition. Interestingly, the initial kinetic friction force F_k has a local maximum near L_c. However, after the transition the maximum in F_k disappears.

Steady-State Sliding. In general, Figures 6 and 7 show that, in the steady state, both F_s and the stick−slip amplitude $\Delta F = F_s - F_k$ increase with load. If one wanted to fit a line through the data points after the transition to obtain the steady-state friction coefficient, μ, very different values would be obtained for the static and kinetic values, μ_s and μ_k. Moreover, different values would be deduced depending on whether one defines the friction coefficient in terms of the chord (F/L) or the slope (dF/dL) of the force vs load curve where, generally, $F/L > dF/dL$. Even then, the values obtained are not at all constant but depend on the load and sliding velocity. Thus, the concept of a characteristic friction coefficient does not appear to be valid for such systems. However, to enable comparison with literature values for solids sliding on polymers, a ballpark figure of $\mu_s \approx 1.0-2.0$ is obtained for F_s/L, and $\mu_s \approx 0.3$ is obtained for dF_s/dL, both at high loads. In contrast, the corresponding values for the steady-state kinetic friction at high loads are much lower and closer to $\mu_k \approx 0.01$. Above the critical velocity v_c, where the static and kinetic friction forces merge into one value $\mu = \mu_s = \mu_k$, the mean friction coefficient μ was not accurately measured (cf. dashed line in Figure 6) but at high loads was of order $\mu \approx 1.0$. These values may be compared with the literature values on similar systems.[18] Thus, for polycarbonate sliding on Nylon, the static and kinetic friction coefficients are $\mu_s = 0.25$ and $\mu_k = 0.04$.[16,17] For other systems involving steel sliding on various polymers, the friction coefficients μ for steady-state sliding above v_c fall between 0.1 and 0.7.[17]

Figure 8 illustrates the temperature dependence of the kinetic friction F_k as a function of the sliding cycle, N, or sliding time, t. The measurements were performed at a low load of $L = 5$ mN. The dynamic response of the system is clearly different above and below the (bulk) glass transition temperature of 25 °C. Below the glass transition temperature, F_k remains almost constant for the first few sliding cycles, then decreases rapidly during the transition. The closer the temperature gets to T_g, the earlier the transition occurs. Above T_g, the kinetic friction force is already much reduced by the end of the first sliding pass ($N = 1$). This trend is shown in the inset of Figure 8 and strongly suggests a thermally activated (diffusion-type) mechanism for the transition from rest to steady-state sliding.

Parameters that Define the "Massaging" Transition. Figure 9 reveals some crucial insights into the transition from rest to steady-state sliding, namely, that it depends on the number of cycles or the total distance traveled but not on the driving velocity, which further implies that it does not depend on the *time* of sliding. The question of whether a surface or

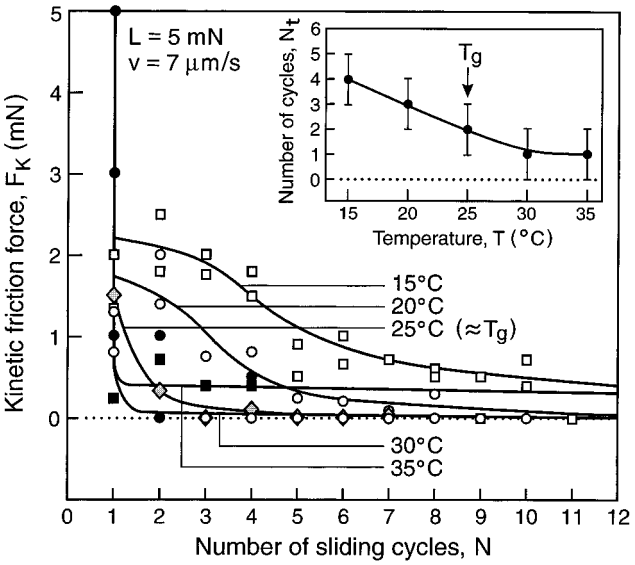

Figure 8. The kinetic friction F_k versus the number of sliding cycles N, where each cycle corresponds to a sliding distance of 1000 μm (1 mm). The different curves illustrate the transition to steady-state sliding at different temperatures from 10 °C below to 10 °C above the glass transition temperature, $T_g \approx 25$ °C. At lower temperatures, the transition takes longer, whether measured in time, distance slid, or number of cycles passed. The inset shows how the number of cycles in the transition N_t decreases with temperature. Above T_g, $N_t \approx 1$, so the transition either takes place during the first sliding pass or there is no transition, steady-state sliding conditions being attained immediately.

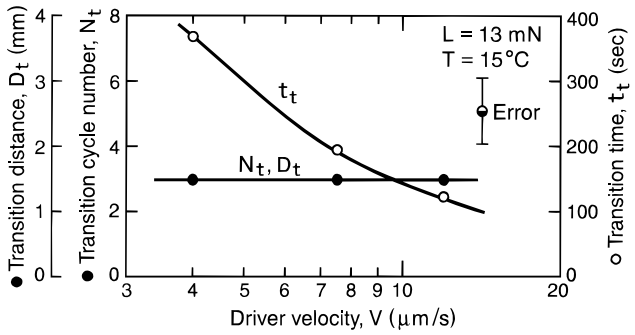

Figure 9. Number of sliding cycles N_t and total distance traveled D_t in the transition to steady-state sliding as a function of the driver velocity, V. Also shown is the transition time, t_t, as a function of V. The apparent constancy of N_t and D_t, even as the sliding *time* of the transition changes, shows that the transition does not depend on some characteristic relaxation time or slider velocity but on the number of cycles (passes) or total sliding distance.

interface has to be sheared for a certain (characteristic relaxation) *time* or over a certain *distance*, or some other characterizing factor, before it adapts to new sliding conditions depends on the tribological system. The transitions of most simple liquid lubricants appear to be describable in terms of a characteristic relaxation *time*,[10] whereas hard, unlubricated surfaces with multiple contacts are better described by a characteristic "massaging" *distance*.[18] In some cases, for example, where branched low MW polymer liquids act as lubricant fluids, sliding has to proceed both over some characteristic time τ_c *and* distance D_c for the transition to be complete.[15] Both of these parameters are generally interdependent, and they also depend on the sliding conditions such as the load, velocity in relation to $V_c = D_c/\tau_c$, temperature, and previous history, and it is therefore often difficult to unambiguously distinguish between them. In addition, other relaxation times and distances may occur in a complex fluid system, which is tantamount to having more than

one Deborah number, each having different values for τ_c and D_c. Clearly, the complete transition from rest to steady-state sliding will involve relaxations at all these time and distance scales, but the longest τ_c and D_c values will determine when the transition is complete. In the present experiments, we may conclude that sliding has to proceed over a distance x_{tot} corresponding to three passes of the mica surface across the polymer surface before the polymer molecules have settled into their final dynamic configuration. Given the asymmetric geometry of this system (cf. Figure 1b), the massaging distance is therefore approximately 3 times the contact diameter, viz. $x_{tot} = 3 \times 50 = 150\ \mu$m. This is much greater than the molecular size, entanglement length, asperity, or domain size, or even the contact diameter of the sliding junction. Alternatively, since the total sliding distance is proportional to the number of cycles needed to reach steady-state sliding conditions, it could be that the number of passes or cycles, N, determines the transition.

In conclusion, the data point to at least two relaxation mechanisms and to a characteristic sliding *distance*, but not *time*. Additional data is presented to support both of these conclusions in the accompanying paper,[1] and the question of the likely molecular processes occurring during the transition is considered in the Discussion and further developed in ref 1.

Adhesion Measurements. The dynamic adhesion forces were also measured as a function of contact time. For contact times of order 1−5 min at $T = 17.3$ °C, the measured adhesion force needed to separate two asymmetric surfaces (of radii $R = 1.3$ cm) from contact was $L_s \approx 25 \pm 5$ mN, which gives for the effective work of adhesion or adhesion energy[19]

$$W_{eff} = W_s = 2L_s/3\pi R \approx 400\ \text{mJ/m}^2 \qquad (3)$$

This value is significantly higher than the equilibrium (thermodynamic) value which, assuming that the mica−PnBMA adhesion is determined mainly by the van der Waals forces between them, may be estimated[19,20] to be of order $W_0 \approx 2(\gamma_{mica}\gamma_{polymer})^{1/2} \approx 2(66 \times 31)^{1/2} \approx 100$ mJ/m^2. Any nonequilibrium effects usually lead to higher effective values for W_s than the equilibrium thermodynamic value, and this enhanced adhesion is often closely related to the friction forces, as discussed below.

It was also noted that if the surfaces are separated (normally) while subjected to a finite shear force, F (where $F < F_s$), the adhesion or pull-off force is less than the (maximum) value obtained at $F = 0$. The pull-off force was found to be reduced from the maximum value by $\sim 0.75F$. For example, under a shear force of ~30 mN, the adhesion force at pull-off had fallen from L_s ~30 to ~10 mN.

Transfer Film. As already mentioned, there was no change in the polymer film thickness during transitions to steady-state sliding at temperatures less than $T_g + 20$ °C. However, starting from 25 °C above T_g and up, the MBI fringes coming from the contact zone become increasingly distorted, indicative of major structural changes. Initially, at 20−25 °C above T_g, the straight fringes become wavey but remain centered at the same wavelength, indicating that the polymer surface becomes rippled at constant average film thickness. At $T_g + 30$ °C, the fringes showed that polymer material was accumulating preferentially in the middle of the contact area, and by $T_g + 35$ °C there was evidence of material transfer out of the contact area, which was now also visible when looking directly at the surfaces from the top using an optical microscope. We describe these effects in more detail in our follow up paper.[1]

We also looked for any evidence of polymer transfer from one surface to the other. First, we measured the surface topography of both surfaces by MBI and AFM before and after sliding and found no evidence of material transfer; the mica surface remained molecularly smooth and quite unlike the PnBMA surface. Second, we looked for evidence of transfer during friction experiments as follows. After the transition to steady-state sliding had occurred, we slid the mica surface "out of its track", i.e., into virgin polymer region. Once out of its track, the friction changed to the same value as the initial friction, i.e., to the pre-transition value, but it immediately returned to the post-transition value on sliding the mica surface back into the track. This observation does not exactly exclude a molecular transfer film, but it strongly suggests that, if there is one, it is not responsible for the observed transition. Transfer films *were* observed at temperatures in excess of 20−25 °C above T_g where PnBMA is softer. We describe our transfer measurements in detail in the second MS.[1]

Discussion and Conclusions

The glass transition is a second order transition which typically extends over 20°C, that is, roughly ±10 °C on either side of T_g. Our measurements should therefore be thought of as having been conducted at T_g, rather than above or below T_g. At T_g, polymers are often thought of as behaving more like liquids than solids, although this depends on the characteristic measuring time, i.e., the shearing frequency or sliding velocity. Our previous work on the adhesion dynamics of PnBMA surfaces near T_g[9] showed it to be highly mobile and more liquidlike than a hard inorganic or metallic surface, an elastomer, or even a glassy polymer.

But the results presented here on the tribological properties of PnBMA reveal behavior at T_g that does not fall neatly into either category (liquidlike or solidlike). For example, the friction is quite high and exhibits stick−slip and long relaxation times, which is quite different from highly fluid surfaces that have low friction, no stick−slip, and fast relaxation times.[10,33] They are also quite different from hard (brittle), rubbery, or elastic surfaces which display little velocity or memory-time effects but do appear to have but a characteristic "memory-distance" (cf. the recent tribological experiments on PMMA well below its T_g by Baumberger et al.[18]).

Adhesion−Friction Relationship. We first consider the relationship between the *friction* and *adhesion* mechanisms of the mica−PnBMA system. As already mentioned, nonequilibrium, hysteretic, or time-dependent adhesion forces are generally related to the friction forces. Indeed, when the adhesion and friction energy dissipation mechanisms are the same, the friction force F is related to the hysteresis in the adhesion energy ($W_{eff} - W_0$) by[10]

$$F = \mathrm{A}(W_{eff} - W_0)\epsilon/2\sigma \qquad (4)$$

where W_{eff} (the effective surface energy) is related to the measured pull-off force by eq 3, W_0 is the equilibrium surface energy ($W_0 \approx 100$ mJ/m^2), A is the contact area during sliding, σ ($\approx D_c$) is the characteristic dimension of the energy dissipating mechanism, and ϵ is the energy transfer efficiency per collision. We expect $\epsilon = 1$ for the static friction, and $\epsilon < 1$ for the kinetic friction.

Equation 4 has been found to work well for a variety of different surfaces[4,21−23] in which σ is of order 1 nm, i.e., close to a molecular dimension. In the case of polymer surfaces, larger-scale molecular domains may be involved.[8] Indeed, using the experimentally measured values: $F \approx 50$ mN, $W_{eff} - W_0 \approx 300$ mJ/m^2, $\mathrm{A} = \pi r^2 = \pi(25 \times 10^{-6})^2 = 2 \times 10^{-9}$ m^2, and

assuming $\epsilon = 1$, we obtain $\sigma \approx 5-10$ nm. As previously noted for polymer surfaces,[8] the characteristic length scale σ associated with friction processes may be larger than a molecular dimension. This is also consistent with the stick−slip friction results presented here which indicate that large length scales, defined as D_c, may be involved in the energy dissipation processes, and it is also supported by our recent results on the surface deformations associated with the adhesion dynamics of PnBMA surfaces.[9]

In light of the above analysis and previous modeling of stick−slip friction,[10] it is apparent that, during the slip, the kinetic friction is very much lower than the static friction, perhaps as low as 0.01 of F_s. This suggests that during the slip the interface either "melts"[24] or that the surface molecular groups become oriented in an ordered "superkinetic" sliding configuration.[25] These molecular mechanisms are explored further below.

At steady-state sliding, the *mean* friction force (being the average of the static and kinetic values) under different sliding conditions corresponds to friction coefficients of the order 0.3−1.0, which is very similar to literature values ($\mu = 0.1-0.7$) for various solids sliding on various polymer substrates.[17]

Molecular Ordering at the Shearing Interfaces. We now focus on the molecular mechanisms responsible for the observed friction behavior. Briefly, the results show that for a solid surface of mica sliding on a stationary surface of PnBMA at temperatures close to T_g, the friction is of the stick−slip type at sliding velocities below the critical velocity, $v_c \approx 10$ μm/s, and becomes smooth at higher sliding velocities. In the stick−slip regime, the kinetic friction force decreases to a very low value after the commencement of sliding (the rate of decrease depending sensitively on the temperature), whereas the static friction force remains largely unchanged at its initial high value. On stopping and restarting in the steady-state sliding regime, the kinetic friction remains at its low value even for stopping times of many hours (so long as the surfaces remain in contact throughout the stopping period).

This behavior is somewhat different from that observed with simple liquid or solid surfaces or films in a number of ways: (1) the transition from rest to steady-state sliding involves a slow but dramatic decrease in the kinetic friction force but not the static force; (2) there is no rapid relaxation of the kinetic friction force back to the initial state on stopping; (3) more than one relaxation process may be operating, one of which appears to have a large characteristic length scale; (4) the relaxation to steady-state sliding is not characterized by a simple relaxation *time* but depends on the sliding distance or number of passes made. In addition, we note that the adhesion force is significantly higher, by a factor of about 4, than the equilibrium value. This factor is similar to the enhanced adhesion of amorphous surfactant monolayer-covered surfaces[26] and polymer surfaces in the glassy or cross-linked state,[27] but much less than the factor of ∼100 obtained for the symmetric configuration of two PnBMA surfaces adhering to one another,[9] although in this latter case the polymer layers were much thicker (∼2 μm) allowing for bulk flow effects to occur that also contributed to the adhesion hysteresis.

Proposed Model of the Shearing Solid-on-Polymer Interface. The following model, illustrated in Figures 10 and 11, appears to explain all of the observed trends and may also apply to other polymer−surface systems. The model is consistent with the tribological data and the known molecular structure and properties of PnBMA, although some of the molecular-scale details, such as how the molecules' backbones and side groups

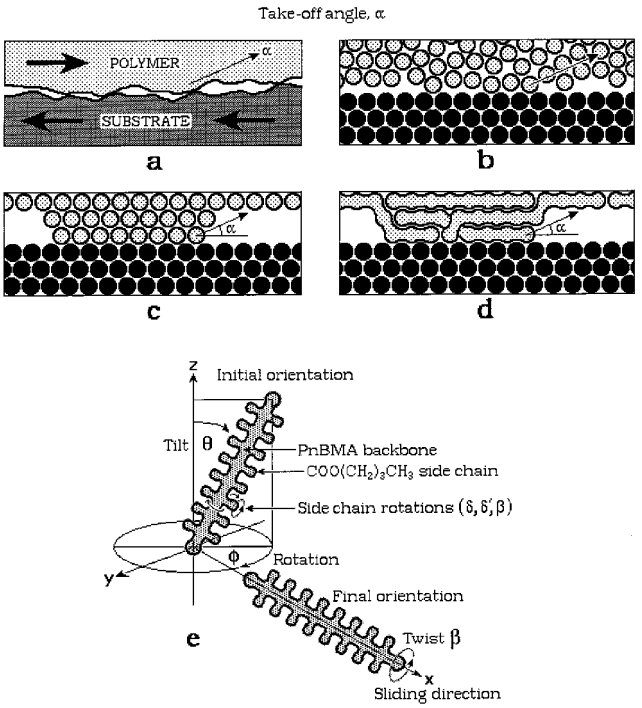

Figure 10. (a−d) Macroscopic surface deformations and molecular scale reordering occurring at a shearing asymmetric interface of two dissimilar materials which do not lead to a change in the static "takeoff" angle α. In such cases, the static friction force F_s will not change but the kinetic force F_k may change significantly. (Figures adapted from refs 4 and 28 for symmetric surfaces.) (e) Molecular structure of PnBMA showing (part of) the polymer backbone and side chain segments which protrude out from the backbone by ∼10 Å. Also shown are the various angles of rotational freedom available for the backbone and side chains, which together determine the takeoff angle α.

contort during sliding, illustrated in Figure 11, are of a more speculative nature.

The results show that there must be at least two different molecular rearrangement or relaxation processes, a fast one and a slow one. The slow one does not alter the static friction but reduces the dynamic friction significantly.[34] Parts a and b of Figure 10 (adapted from refs 4 and 28) show how macroscopic and molecular restructuring at a surface can still produce the same static friction force, F_s, which depends on the *static* surface geometry or topography and particularly on the "takeoff angle", α. As discussed in two previous papers on the stick−slip friction of fluorocarbon monolayers and C_{60} surfaces,[4,28] α can remain largely unchanged even after drastic molecular reorientations have taken place involving either macroscopic (a) or molecular-scale (b, c, d) reordering.

In contrast, the kinetic friction force F_k is much more sensitive to subtle changes in the local topography. This is because F_k depends on the energy exchange/transfer efficiency of colliding molecules or asperities during the rapid slip part of the stick−slip cycle, represented by the factor ϵ in eq 4, which is affected by such *dynamic* factors as the slip time and velocity and the inertia (mass, local stiffness, and vibration frequency) of the colliding surface molecular groups or asperities.[10] Thus, without going into specific details, one can see how molecular rearrangements at a shearing interface may allow F_s to remain (roughly) constant as F_k changes.

Concerning the specific system of PnBMA sliding on mica, one should note that poly(*n*-alkyl methacrylates) in general are well-known for their particularly long $(CH_2)_n$ side chains, approximately 10 Å long when fully stretched, which exhibit three bulk relaxation modes (Figure 10e): two "internal"

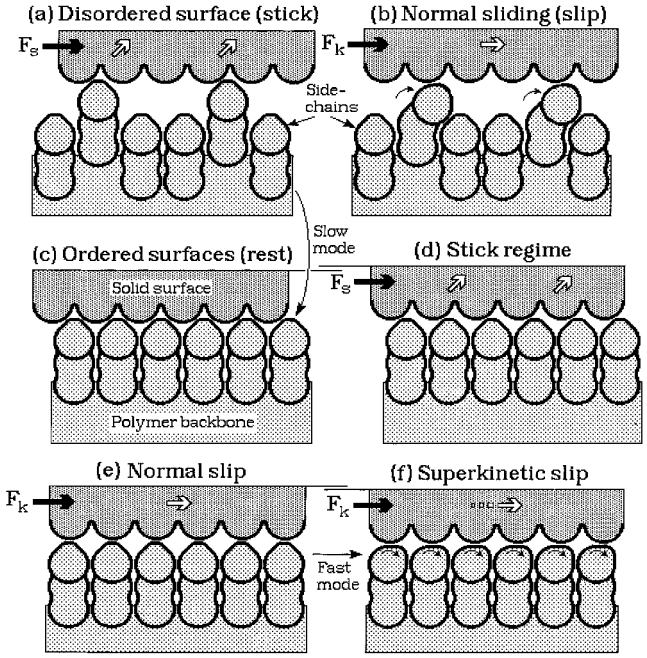

Figure 11. Proposed molecular rearrangements occurring during steady-state stick−slip sliding for a solid crystalline surface (e.g., mica) sliding across a polymer surface (e.g., PnBMA) at $T \approx T_g$ (see also Figures 5 and 10). Panels a and b show the conditions at the surfaces before the "massaging" transition. Panels c−f show the conditions after the transition, i.e., during steady-state sliding. The surfaces have the same static friction in both cases due to the same takeoff angle, α (white arrows), but the kinetic friction is much lower. Panel f shows two possible transient configurations during "superkinetic" slip: the outermost surface groups may tilt to provide an ultralow "superkinetic" friction state[4,25] or the surface layer may "melt", thereby producing the same effect.[24]

rotational modes, δ and δ', and the β mode which arises from rotations of the side chain as a whole.[29−31] The δ and δ' modes have activation temperatures of ∼125 K so that at near ambient temperatures the side chains are expected to be fully activated, especially at the surface. The polymer backbone motion, however, remains confined up to $T \approx T_g$.

Provided that the side chain-to-backbone ratio is not significantly different at the polymer surface from that in the bulk, we may expect ∼80% of the surface groups to be the PnBMA side chains. Therefore, they are expected to play a dominant role in frictional energy loss mechanisms. On the basis of the known structure of PnBMA, we can discuss the tribological behavior of this system in terms of a simplified molecular model consisting of two main relaxation or entanglement modes: the first (fast mode) involving the side chain angles δ, δ', and β, and the second (slow mode) involving the tilt and rotational angles θ and ϕ of the polymer backbone (Figure 10e). From our results, these two modes must have time constants that differ by at least 2 orders of magnitude.

Our results also reveal that the kinetic friction force decreases as the number of cycles N increases. In other words, the ability of the molecules to go into a dynamic friction configuration is increased under the repeated "massaging" of the polymer by the rigid solid surface of the mica slider. The molecular configuration of the polymer molecules at the surface is thus successively modified with increasing N to allow for ever more favorable molecular orientations during sliding, but without affecting the static friction force (or angle α). The most obvious candidates for this slow massaging or adaptation mode are, of course, the orientations of the backbone, defined by angles θ and ϕ.

The above model differs from previous friction models in having two relaxation modes that are not independent, but coupled. Thus, initially, the molecules at the interface are not shear-ordered and can be only partially "flipped" into the fast (superkinetic) relaxation mode (Figure 11, a → b). The repeated massaging by the mica slider leads to a more ordered backbone configuration (Figure 11c), which has the same takeoff angle and hence the same static friction force (Figure 11d), but a lower activation threshold for the fast relaxation mode, i.e., the side chains can flip more easily into the slip configuration (Figure 11, d → e → f).

Since our results show that the number of cycles needed to reduce F_k is extremely sensitive to the temperature near T_g (cf. Figure 8), we may conclude that the activation process underlying the slow relaxation mode is closely linked to the glass transition of PnBMA.[31]

Finally, the model can account for the reduced adhesion force measured when the surfaces are separated while subjected to a lateral or shear force. From parts c and d of Figure 11, we see that as the lateral force is increased toward F_s, the surface molecules move farther apart, i.e., the interface dilates elastically, and the number of van der Waals bonds or contacts across the interface decreases. This is consistent with the observed linear decrease in the pull-off force by roughly the same amount as the applied lateral force (see Results). This example of a separation from "dry solid" contact is in contrast to the case of two mica surfaces sliding with a thin fluid lubricant film between them (exhibiting smooth sliding without stick−slip) where the pull-off force does not depend on the shear force, but remains at the same value even when the surfaces are separated during sliding.[10] This model and its implications are discussed further in the adjoining paper on the complementary system of polymer sliding on mica.[1]

Acknowledgment. This work was supported by the DOE under Grant DE-FG03-87ER45331 (M.H., G.L., and J.N.I.) and the Swiss National Research Fund (M.H.).

References and Notes

(1) Luengo, G.; Heuberger, M.; Israelachvili, J. In preparation.

(2) Kumacheva, E. *Prog. Surf. Sci.* **1998**, *58*, 75. Klein, J. *Ann. Rev. Mater. Sci.* **1996**, *26*, 581.

(3) Luengo, G.; Schmitt, F.-J.; Hill, R.; Israelachvili, J. *Macromolecules* **1997**, *30*, 2482.

(4) Yamada, S.; Israelachvili, J. *J. Phys. Chem. B* **1998**, *102*, 234.

(5) Ruths, M.; Granick, S. *J. Phys. Chem. B* **1998**, *102*, 6056. Dhinojwala, A.; Cai, L.; Granick, S. *Langmuir* **1996**, *12*, 4537.

(6) Tabor, D. In *Advances in Polymer Friction and Wear*; Lee, L-H., Ed.; Polymer Science and Technology, Vol. 5A; Plenum: New York, 1974. Biswas, S. K.; Vijayan, K. *Wear* **1992**, *158*, 193. Spalding, M. A.; Kirkpatrick, D. E.; Hyun, K. S. *Polym. Eng. Sci.* **1993**, *33*, 423.

(7) Ferry, J. D. *Viscoelastic Properties of Polymers*, 3rd ed.; Wiley: New York, 1980. Becker, M. E.; Kilian, R. A.; Kosmowski, B. B.; Mlynski, D. A. *Mol. Cryst. Liq. Cryst.* **1986**, *132*, 167.

(8) McLauren, K. G.; Tabor, D. *Nature* **1963**, *197*, 856. Grosch, K. A. *Nature* **1963**, *197*, 858. McLauren, K. G.; Tabor, D. *Proc. R. Soc. London* **1963,** *A274*, 21.

(9) Luengo, G.; Pan, J.-M.; Heuberger, M.; Israelachvili, J. N. *Langmuir* **1998**, *14*, 3873.

(10) Berman, A.; Israelachvili, J. N. In *CRC Handbook of Micro/Nanotribology*, 2nd ed.; Bhushan, B., Ed.; CRC Press: Boca Raton, New York, 1999; Chapter 9, p 371. Berman, A.; Israelachvili, J. N. *Isr. J. Chem.* **1995**, *35*, 85.

(11) Heuberger, M.; Luengo, G.; Israelachvili, J. *Langmuir* **1997**, *13*, 3839.

(12) Reiner, M. *Phys. Today* **1964**, January, 62.

(13) Berman, A.; Ducker, W.; Israelachvili, J. N. *Langmuir* **1996**, *12*, 4559. Berman, A. D.; Ducker, W. A.; Israelachvili, J. N. In *Physics of Sliding Friction*; Persson, B., Tosati, E., Eds.; NATO Advanced Science Institute Series; Kluwer Academic Publishers: Dordrecht, 1996; Chapter 3, p 51.

(14) Yoshizawa, H.; Israelachvili, J. *J. Phys. Chem.* **1993**, *97*, 11300.

(15) Drummond, C.; Israelachvili, J. Unpublished results.

(16) In the literature, the term "kinetic friction" can refer either to the steady-state friction force during smooth sliding at constant velocity or to the lowest friction force reached at a end of a slip during stick−slip sliding. The former depends on V but is independent of the inertia of the moving stage, whereas the latter is a transient value that depends on V but also on the mass of the stage, m, and the stiffness of the friction-force measuring spring, k_F. This distinction is important when making comparisons between different types of experiments or between quoted values for the static and kinetic friction coefficients. In the experiments described here, we measured both types of kinetic friction, one above the critical velocity, v_c, the other below v_c. The kinetic friction measured during stick−slip is therefore not the true kinetic friction, but it does scale (nonlinearly) with it since m and k_F remained the same throughout these experiments. Some recent papers (e.g., ref 13) have analyzed how the "true" kinetic friction force law, $F(V)$, as a function of velocity V can be extracted from a stick−slip friction trace in terms of the measured F_s, F_k, m, k_F, the stick−slip frequency and spike shape.

(17) *Handbook of Tribology: Static and Kinetic Friction Coefficients for Selected Materials*; Table 3, p 73.

(18) Baumberger, T.; Caroli, C.; Perrin, B.; Ronsin, O. *Phys. Rev. E* **1994**, *49*, 4973. Dieterich, J. H.; Kilgore, D. *Pure Appl. Geophys.* **1984**, *43*, 283. Berthoud, P.; Baumberger, T.; G'Sell, C.; Hiver, J.-M. *Phys. Rev. B* **1999**, *59*, 14313. Baumberger, T.; Berthoud, P.; Caroli, C. *Phys. Rev. B* **1999**, *60*, 3928.

(19) Israelachvili, J. *Intermolecular and Surface Forces*, 2nd ed.; Academic Press: London, Orlando, 1991.

(20) The van der Waals dispersion force contribution to the surface energy of mica, based on the measured Hamaker constant of $A = 1.35 \times 10^{-19}$ J, is 66 mJ/m^2. The measured value for PnBMA at 20 °C is 31.2 mJ/m^2 [Wu, J. *Phys. Chem.* **1970**, *74*, 632−638]. The equilibrium adhesion energy for PnBMA with mica is therefore expected to be[19] $W_0 \approx 2(\gamma_{mica}\gamma_{PBMA})^{1/2} = 2(66 \times 31)^{1/2} = 90$ mJ/m^2. According to these values, and using the Young−Dupré equation, $\gamma_{PBMA}(1 + \cos\theta) = W_0$, the contact angle θ of liquid PnBMA on mica should be 0°, i.e., it should spread on mica. Contact angle measurements in our lab show that a droplet of liquid PnBMA (at $T \gg T_g$) does indeed spread on mica, then retracts to a lens on a thin wetting film of PnBMA at an angle of $\theta \approx 14°$.

(21) Israelachvili, J.; Chen, Y.-L.; Yoshizawa, H. In *Fundamentals of Adhesion and Interfaces*; Rimai, D. S.; DeMejo, L. P.; Mittal, K. L., Eds.; VSP: 1995; p 261.

(22) Schmitt, F.-J.; Yoshizawa, H.; Schmidt, A.; Duda, G.; Knoll, W.; Wegner, G.; Israelachvili, J. *Macromolecules* **1995**, *28*, 3401.

(23) Vigil, G.; Xu, Z.; Steinberg, S.; Israelachvili, J. *J. Colloid Interface Sci.* **1994**, *165*, 367.

(24) Thompson, P.; Robbins, M. *Science* **1990**, *250*, 792. Robbins, M.; Thompson, P. *Science* **1991**, *253*, 916.

(25) Yoshizawa, H.; McGuiggan, P.; Israelachvili, J. N. *Science* **1993**, *259*, 1305.

(26) Chen, Y. L.; Helm, C.; Israelachvili, J. N. *J. Phys. Chem.* **1991**, *95*, 10736.

(27) Merrill, W. W.; Pocius, A. V.; Thakker, B. V. *Langmuir* **1991**, *7*, 1975. Watanabe, H.; Tirrell, M. *Macromolecules* **1993**, *26*, 6455. Mangipudi, V. S.; Tirrell, M.; Pocius, A. V. *J. Adhes. Sci. Technol.* **1994**, *8*, 1251. Mangipudi, V. S.; Huang, E.; Tirrell, M.; Pocius, A. V. *Macromol. Symp.* **1996**, *102*, 131. Deruelle, M.; Léger, L.; Tirrell, M. *Macromolecules* **1995**, *28*, 7419. Falsafi, A.; Deprez, P.; Bates, F. S.; Tirrell, M. *J. Rheol.* **1997**, *41*, 1349.

(28) Luengo, G.; Campbell, S. E.; Srdanov, V. I.; Wudl, F.; Israelachvili, J. N. *Chem. Mater.* **1997**, *9*, 1166.

(29) Willbourn, A. H. *Trans. Faraday Soc.* **1950**, *54*, 717.

(30) Garwe, F.; Schönhals, A.; Beiner, M.; Schröter, K.; Donth, E. *J. Phys.: Condens. Matter* **1994**, *6*, 6941. Domberger, W.; Reichert, D.; Garwe, F.; Schneider, H.; Donth., E. *J. Phys.: Condens. Matter* **1995**, *7*, 7419.

(31) Shimizu, K.; Yano, O.; Wada, Y. *J. Polym. Sci.* **1975**, *13*, 1959.

(32) Beiner, M.; Garwe, F.; Schröter, K.; Donth, E. *Polymer* **1994**, *35*, 4127. These authors reported a shear-induced aging process on PnBMA, measured in a rheometer. They observed an increase of the mean relaxation time of at least 2 orders of magnitude with aging below T_g.

(33) Granick, S. *Science* **1991**, *253*, 1374. Van Alsten, J.; Granick, S. *Macromolecules* **1990**, *23*, 4856.

(34) Strictly, even the static friction force, F_s, is never a true static force but depends on the sliding velocity. This is due to the fact that there is already some creep relaxation during the initial "stick" part when the lateral force is being increased from zero to the critical value (cf., Figure 3) over a necessarily finite time that depends on the driver velocity V and spring stiffness K_F. Since this time is shorter at higher V, so F_s is generally slightly *higher*, as observed in Figure 6, because there is less time for creep relaxation to occur.